Interface-State Density in SOI-FET Sensors

O.V. NAUMOVA, B.I. FOMIN
Russian Academy of Sciences, Siberian Branch
A.V. Rzhanov Institute of Semiconductor Physics
Novosibirsk, Lavrent’eva Avenue, 13
RUSSIA
naumova@isp.nsc.ru

Abstract: - SOI-FET sensors are high-sensitivity analytical devices used for qualitative and quantitative analyses of biological and chemical substances. Decreasing and monitoring of the state density at surface of sensors are the key tasks to increase their sensitivity and reproducibility of parameters of devices. This study aims to apply the threshold voltage method to the SOI-FET sensor/electrolyte systems to determine the density of states in the sensors. For this aim: 1) a dependency between the sensor threshold voltage and the voltage on the electrode immersed in the electrolyte solution was derived, 2) the analytical and experimental dependencies were used to determine the density of states at the sensor surface D_{it}, 3) errors in D_{it} related to the uncertainty of values of components of the electrolyte capacitance were determined. It was shown that the uncertainty in the D_{it} values can be estimated in the process of measuring in solutions with various salt concentrations (1-100 mM). The maximal error in D_{it} related to the uncertainty of capacitance associated with the charge adsorbed on the sensor surface Q_{ad} can be estimated using the well-known design parameters of sensor, the salt concentration in solution and Q_{ad}=0. In particular, it was shown that for sensors with typical parameters (the buried oxide thickness of 200 nm, sensor thickness of 30 nm and top-oxide thickness of 2 nm) this error in D_{it2} does not exceed 40% in the 100 mM buffer solutions. The threshold voltage method can be successfully applied for monitoring D_{it} at the stage of cleaning and activation of the sensor surface.

Key-Words: - interface-state density, biosensor, silicon-on-insulator, field-effect transistor

1 Introduction

It is well known that silicon-on-insulator (SOI) strips or nanowires with ohmic contacts provided at their ends are high-sensitivity sensing elements due to the high surface-volume aspect ratio. Compatibility of their manufacturing with current silicon CMOS- technology provides a possibility of fabrication of the System-on-Chip Integrated Circuits with a huge potential for a large variety of chemical and biomedical applications. Nowadays, such sensors are employed for detection of single viruses [1], or proteins [2-5], DNA [3, 3, 6], RNA [2, 3, 7], and other target particles with extremely low (10^{-13}-10^{-16} M) concentration in solutions.

The localization of sensor element on a buried oxide (BOX) of SOI-structure makes this sensor a double gate field effect transistor (SOI-FET), where BOX is used as a bottom gate oxide, the substrate of the silicon-in insulator structures is used as a bottom gate (BG). A bottom-gate voltage V_{bg} induces a conducting channel near the SOI/BOX interface and allows to choose the optimal operation mode (the subthreshold or depletion mode for SOI-FET) to obtain maximum response to adsorbed particles [8, 9]. Any particles adsorbed on the sensor surface act as a second virtual gate, causing a change in conductivity in the SOI-FET sensor due to the so-called coupling-effect - coupling of potentials at the opposite sides of SOI depletion layer [10].

Typically, surface of sensors is covered by oxide (native, thermally or chemically grown). It is obvious, that a high density of states at the Si/top-oxide interface leads to a screening of the charge of the adsorbed target particles. Therefore, monitoring and decreasing of the interface-state densities are the key tasks an increase of sensitivity of sensors and reproducibility of their parameters on a chip.

The threshold voltage method can be used for testing interface-state density in standard SOI-FETs [10]. The aim of this study is to use this method for SOI-FET sensor/electrolyte systems. For this purpose, in Section 2 we discuss the threshold voltage method and the problems associated with its applying to the SOI-FET sensor/electrolyte systems. In Section 3, an analytical solution of the equations for the sensor/electrolyte system to relate the threshold voltage of sensor and voltage on the electrode immersed in electrolyte (top gate, TG) was shown. An equivalent circuit for the top-gate portion of SOI-FET sensor in electrolyte was used for this solution. The threshold voltage method based on the established dependency was applied to SOI FET sensors with different type of surface preparation (with 2 nm oxide on the surface, after activation and covering of the sensor surface by carbonyldiimidazole). In addition, conditions for estimation of errors related to the uncertainty of parameters (components of capacitance) of electrolyte are considered in this report.

2 Problem Formulation

For a standard SOI-FET, the interface-state density can be determined using the approach by Lim and Fossum stated in report [10], where the potential coupling between top (or front) and bottom (or back) gates of thin-film SOI was analyzed.

Fig.1a illustrates a four-terminal SOI-FET structure and the drop of potentials in transistor. In the model by Lim and Fossum, the back (ψ_1) and front (ψ_2) surface potentials are the band bending from a hypothetical neutral film-body point to the respective surface [10]. The electrostatic potential at this point, if source is grounded, is just the build-in potential of the source-film body. Than in analogy to bulk MOSFET theory the back-gate V_{bg} and top-gate V_{tg} voltages can be written as:

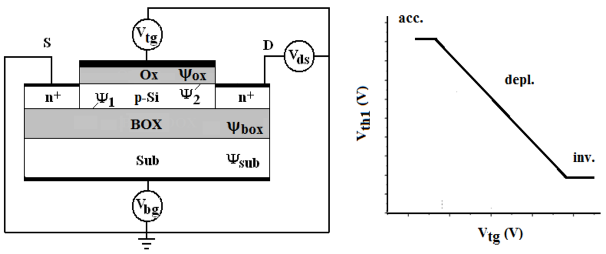

a b

Fig.1. Cross-sectional diagram of a standard n-channel SOI-FET and drop of potentials across transistor - (a), schematic presentation of $V_{th1}(V_{bg})$ curve for a completely depleted SOI FET - (b).

$$V_{bg} = \psi_{sub} + \psi_{box} + \psi_1 + \varphi_{ms1} \tag{1}$$

$$V_{tg} = \psi_{ox} + \psi_2 + \varphi_{ms2} \tag{2}$$

Here and below, the subscripts 1 and 2 refer respectively to the Si/BOX (bottom) and Si/Ox (top) interfaces (Fig.1a); ψ_{box} and ψ_{ox} are the potential drops in the BOX and top-gate oxide; φ_{ms} is the gate-body work-function differences; ψ_{sub} is the potential drop in the Si substrate. The solution of Equations (1) and (2) with using Gauss's law for the interfaces, and Poisson's low for the potential coupling between the Si-film interfaces yields the following expressions for V_{bg} and V_{tg}:

$$V_{bg} = V_{fb1} + \left(1 + \frac{C_{it1}}{C_{box}} + \frac{C_{si}}{C_{box}}\right)\psi_1 - \frac{C_{si}}{C_{box}}\psi_2 - \frac{Q_{si}/2 + Q_{c1}}{C_{box}} + \psi_{sub} \tag{3}$$

$$V_{tg} = V_{fb2} + \left(1 + \frac{C_{it2}}{C_{ox}} + \frac{C_{si}}{C_{ox}}\right)\psi_2 - \frac{C_{si}}{C_{ox}}\psi_1 - \frac{Q_{si}/2 + Q_{c2}}{C_{ox}} \tag{4}$$

Here, V_{fb} is the flat-band voltage; $C_{it}=qD_{it}$ is the interface state capacitance; q is the electron charge; D_{it} is the interface-state density; C_{box} is the capacitance of BOX; C_{ox} is the capacitance of gate-oxide; C_{si} is the capacitance of depleted Si-film; Q_{si} is the charge of ionized impurities; Q_c is the carrier charge in Si-film.

Equations (3) and (4) are the key relations that describe the charge coupling between the top- and back-gates when the film body is completely depleted. When the top surface is depleted, ψ_2 is strongly dependent on V_{tg}; its value ranges from about zero to ~2 ψ_B (here, ψ_B is the Si-film Fermi potential) between the onsets of accumulation and inversion, respectively. Combining Equations (3) and (4) leads to the description of the (back-gate) threshold voltage V_{th1} in terms of V_{tg} and device parameters as [10]:

$$V_{th1} \sim \frac{C_{ox}C_{si}}{C_{box}(C_{ox} + C_{it2} + C_{si})} V_{tg} \tag{5}$$

Thus for the depletion mode, the threshold voltage V_{th1} of BG-transistor depends linearly on the top-gate voltage V_{tg}. Fig.1b shows the dependence of V_{th1} on V_{tg} for SOI-FET. Equation (5) and the slope $m=dV_{th1}/dV_{tg}$ of the $V_{th1}(V_{tg})$ dependence are used to determine the interface-state density D_{it2} as:

$$D_{it2} = \left(\frac{C_{ox}C_{si}}{mC_{box}} - C_{ox} - C_{si}\right)/q \tag{6}$$

Fig. 2 shows a cross-sectional diagram of the SOI-FET sensor/electrolyte model system and a sketch illustrating the drop of potentials across this system. Referring to Fig. 1a and Fig.2 it can be seen, that the back-gate voltage V_{bg} is determined by Equation (1) for both the standard SOI-FET and the SOI-FET sensor immersed into electrolyte. It is mean, that Equation (3) is also valid for both devices. However, the top-gate portions of devices differ.

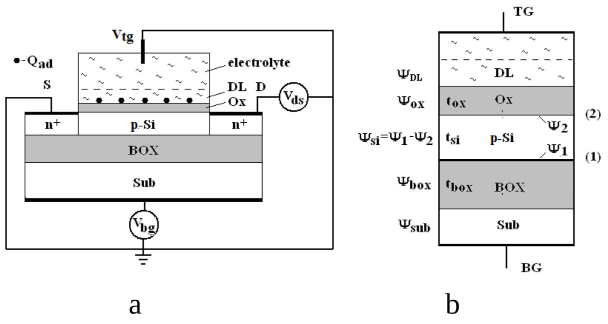

Fig.2. Cross-sectional diagram of the model SOI-FET sensor/electrolyte system - (a), and the potential drops in this system - (b).

According to the site-binding model [11-13] the surface of Si covered by insulator in contact with solution is charged by proton exchange reactions. According to the Gouy-Chapman-Stern model [14, 15], the Stern layer (which has not free charges) lies between the insulator and the diffusion layer of electrolyte with mobile ions. Therefore, the voltage V_{tg} for SOI-FET sensor can be represented as:

$$V_{tg} = \psi_{DL} + \psi_{ox} + \psi_2 + \varphi_{se} \qquad (7)$$

Here, $\psi_{DL} = \psi_{st} + \psi_m$ is the potential drop across the electrolyte double layer (DL); ψ_{st} is the potential drop across the Stern layer; ψ_m is the potential drop across the diffusion layer; ψ_{se} is the Si-electrolyte contact voltage.

Solution of Equation (7) requires: 1) knowledge of the charge density at the sensor/electrolyte interface, which can be determined by the site-binding model, and 2) knowledge of the charge distribution in the diffusion layer, which is obtaining by solving Poisson-Boltzmann equation. Solutions are presented, for example, in reports [13, 15, 16]. However, the results were obtained using numerical algorithms.

Thus, there is no analytical solution the system of Equations (3) and (7) for the fast monitoring of the interface-state density D_{it2} in SOI-FET sensors.

3 Problem Solution

Instead of Equation (7), we used an equivalent circuit for the top-gate transistor in Fig.2 to relate V_{tg} to ψ_2 and eliminate ψ_2 in expression (3).

Fig.3 shows the equivalent circuit for the top-gate portion of SOI-FET sensor in electrolyte. In Fig.3, ψ_o is the potential on the insulator surface; C_{DL} is the total electric double layer capacitance; C_{st} is the Stern-layer capacitance; C_m is the capacitance of the diffusion layer formed by the mobile ions in electrolyte; C_{ad} is the capacitance associated with the adsorbed charge on the insulator surface. In a simplifying picture, Q_{ad} can be seen as the sum two contributions: a negative surface charge mainly due to the ionized silanol groups SiO^- (or the site-binding charge due to the chemical reaction taking place between the pH ions and SiOH groups on the silicon dioxide surface) and a positive Stern-plane charge due to adsorbed cations [13-15]. As a whole the interface charge Q_{ad} is negative for electrolyte with pH>4 [13].

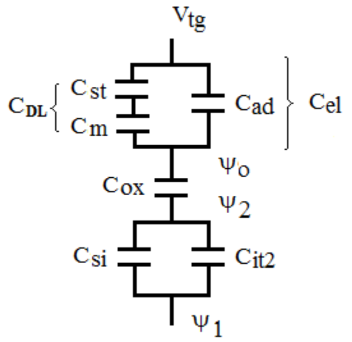

Fig.3. Equivalent circuit for the top-gate portion of SOI-FET sensor. The electrolyte capacitance C_{el} consist of the capacitance C_{ad} associated with the adsorbed charge on the insulator surface in parallel with the Stern-layer capacitance C_{st} and the capacitance of diffuse layer C_m formed due to the mobile ions in electrolyte.

The total electrolyte capacitance C_{el} consist of the electrolyte double layer capacitance C_{DL} in parallel with C_{ad} (Fig.3), i.e,

$$C_{el} = C_{DL} + C_{ad} = \frac{C_{st}C_m}{C_{st} + C_m} + C_{ad} \qquad (8)$$

Referring in Fig.3, for the charges on the serial capacitances we can write:

$$(V_{tg} - \psi_o)C_{el} = (\psi_o - \psi_2)C_{ox}$$
$$= (\psi_2 - \psi_1)(C_{si} + C_{it2} \qquad (9)$$

The solution of Equation (9) yields:

$$\psi_o = V_{tg} - \frac{C_{si} + C_{it2}}{C_{el}}(\psi_2 - \psi_1) \qquad (10)$$

and

$$\psi_2 = \frac{C_{si} + C_{it2}}{C_{si} + C_{it2} + C}\psi_1 + \frac{C_{ox}}{C_{si} + C_{it2} + C_{ox}}\psi_o \qquad (11)$$

On substitution of (10) into (11), we obtain:

$$\psi_2 = \frac{\psi_1}{1+\alpha}\left(\frac{C_{si}+C_{it2}}{C_{si}+C_{it2}+C_{ox}}+\alpha\right) + \frac{C_{ox}}{(1+\alpha)(C_{si}+C_{it2}+C_{ox})}V_{tg} \qquad (12)$$

Here,

$$\alpha = \frac{(C_{si}+C_{it2})C_{ox}}{C_{el}(C_{si}+C_{it2}+C_{ox})} \qquad (13)$$

Substitution of (12) into (3) yields:

$$V_{bg} \sim \frac{C_{ox}C_{si}}{(1+\alpha)(C_{si}+C_{it2}+C_{ox})C_{box}}V_{tg} \qquad (14)$$

Referring in Equations (14) and (8), we can write:

$$\frac{dV_{bg}}{dV_{tg}} \sim \frac{t_{box}, C_{DL}, C_{ad}}{t_{si}, C_{it2}, t_{ox}} \qquad (15)$$

In analogy to the standard SOI-FET, for the depletion mode of SOI-FET sensor the threshold voltage V_{th1} depends linearly on the top-gate voltage V_{tg}. Equation (14) and the slope $m=dV_{th1}/dV_{tg}$ of the experimental $V_{th1}(V_{tg})$ dependence for sensor can be used to determine the interface-state density D_{it2} as:

$$D_{it2} = \left(\frac{C_{ox}C_{si}}{mC_{box}} - C_{ox} - \beta C_{si}\right)/\beta q \qquad (16)$$

Here,

$$\beta = 1 + \frac{C_{ox}}{C_{el}} \qquad (17)$$

Note that the capacitances of the Si and oxide layers used in expression (16) are easy to calculate knowing their thickness (t) and the dielectric constant (ε): $C_{si}= \varepsilon_{si}/t_{si}$, $C_{ox}= \varepsilon_{ox}/t_{ox}$, $C_{ox}= \varepsilon_{ox}/t_{box}$. The capacitance of the Stern layer was set at $2x10^{-5}$F/cm^2 [11, 16]. Yet, the values of the capacitance C_{ad} associated with charge adsorbed on the real sensor surface, and the capacitance of diffuse layer C_m coupled to C_{ad} are never precisely known. Moreover, their values can vary with changing of the V_{tg} voltage. However, we can estimate the impact C_{el} to the D_{it2} value.

It is seen from Equations (16) and (17), when the condition $C_{ox}<<C_{el}$ is satisfied, the coefficient β tends to 1 and the impact C_{el} to D_{it2} can be neglected. When the value of C_{el} is minimal (the worst case), the coefficient β has the maximum value. The impact β to D_{it2} (the error in the determination of D_{it2} due to the uncertainty of the C_{ox}/C_{el} ratio) is maximal.

The C_{el} value is minimal at the minimum values of C_{DL} and C_{ad} – see Equation (8). The electrolyte double layer capacitance C_{DL} consist of the capacitances C_{st} and C_m in series (Fig.3). Assuming that the charge in the diffusion part of electrolyte is screened by the electrolyte ion charges over the Debye length L_D, for the value of the diffusion layer capacitance we can use expression of $C_m=e_{el}/L_D$. Here, $L_D=(kT\varepsilon_{el}/2N_oq^2)^{1/2}$, N_o is the concentration of ions in bulk of electrolyte, k is the Boltzmann's constant, T is the temperature. Note that in (1-100) mM buffer solutions (BS) used mostly in analyzing biological species the L_D thickness ranges from about 1 to 10 nm. It is easy to estimate, that an increase in L_D in the range of (1-10) nm results in an increase of the coefficient β in the range of 1.1-1.4 at t_{ox}=2 nm, C_{ad}=0 and ε_{el}=78.5. For the most commonly used parameters of sensor, the third term in Equation (16) is not dominant. Thus, for sensors with 2 nm thickness of top-oxide, the values of D_{it2} calculated in the worst case (at C_{ad}=0 and L_D=10 nm) can be lower than real by factor ~1.4. This is an acceptable error in the definition of D_{it2}.

In addition, the effect of the electrolyte capacitance on the D_{it2} value was also investigated by varying the concentration of ions in electrolyte. The $V_{th1}(V_{tg})$ dependencies were measured in solutions with the different salt concentration.

In the study, we used n-channel SOI-FET sensors. The sensors were fabricated on p-SOI layers with an acceptor concentration of N_a~$2x10^{16}$ cm^{-3}. The thickness of the top silicon layer amounted to 30 nm. The BOX thickness was 155 or 200 nm. The length of the sensor element was 10 μm, the width was 3 μm. Details of manufacturing of sensors are described elsewhere [8]. A schematic representation of the SOI-FET sensor is shown in Fig.2a.

To determine the $V_{th1}(V_{tg})$ curves, the dependences of the drain current I_{ds} on the voltage V_{bg} were measured upon a variation in the voltage at the top-gate. During all measurements the constant low voltage V_{ds} = 0.15 V was applied between source and drain. The threshold voltages of the SOI-FET sensors were determined by the method of the Y- function (here, $Y=I_{ds}/g_m^{1/2}$, $g_m=dI_{ds}/dV_{bg}$) [17].

Fig.4 shows the $V_{th1}(V_{tg})$ dependencies for SOI-FET sensor in 1 mM (L_D=10 nm) and 100 mM (L_D=1 nm) solutions at pH 7.4. The sensor surface was coated by a 2 nm thick thermal oxide.

Table 1 shows the slope *m* of $V_{th1}(V_{tg})$ curves and the D_{it2} values calculated by Equation (16).

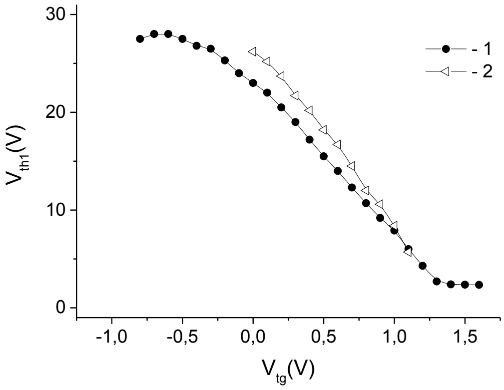

Fig.4. $V_{th1}(V_{tg})$ dependencies of sensor in 1 mM – (1) and 100 mM – (2) BS, pH 7.4. t_{ox}=2 nm; t_{box}=155 nm.

Table 1. Slope m of $V_{th1}(V_{tg})$ dependencies for sensor in solutions with different Debye length L_D, and the D_{it2} values calculated at t_{ox}=2 nm, t_{box}=155 nm, t_{si}=30 nm, and C_{ad}=0.

N	m	L_D, nm	D_{it2}, $eV^{-1}cm^{-2}$
1	16.7	10	$2.6x10^{12}$
2	18.8	1	$3.7x10^{12}$

As expected: 1) the $V_{th1}(V_{tg})$ curves for the sensors have the same shape for the standard SOI-FET (see Fig 4 and Fig.1b), 2) the slope of this curves diminishes, when the Debye length in solution is increase and, correspondingly, the capacitance C_{DL} decreases – see Equation (15), and 3) the difference in the D_{it2} values for 1 mM and 100 mM solutions is quite acceptable (Table 1). We can estimate the D_{it2} values as (3-4) $x10^{12}$ $eV^{-1}cm^{-2}$.

Fig.5 shows the $V_{th1}(V_{tg})$ dependencies for sensors with the different type of the surface preparing. The modification of surface by carbonyldiimidazole (CDI) was applied immediately after cleaning or in 30 minutes after cleaning of the sensor surface. Details of CDI-modification of the sensor surface are described elsewhere [7].

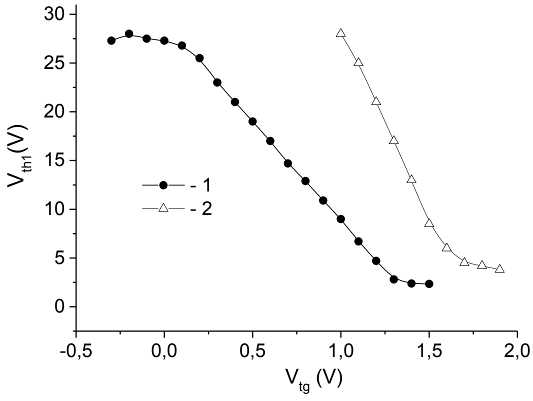

Fig.5. $V_{th1}(V_{tg})$ dependencies of sensors with CDI-coating applied immediately – (1) and in 30 min. after cleaning of surface – (2). 1 mM BS, pH 7.4. t_{ox}=2 nm; t_{box}=200 nm.

Table 2 shows the values of m and D_{it2} for sensors. It is seen that CDI-modification practically does not change the D_{it2} value (cf. Table l and Table 2). However, the delay in modification leads to an obvious increase in the interface-state density.

Table 2. Slope m of $V_{th1}(V_{tg})$ curves and the Dit_2 values calculated for sensors with the CDI-coating applied immediately – (1) and in 30 min after cleaning of surface - (2). The D_{it2} values are calculated at t_{ox}=2 nm, t_{box}=200 nm, t_{si}=30 nm, C_{ad}=0, and L_D=10 nm.

N	m	D_{it2}, $eV^{-1}cm^{-2}$
1	20.7	$2.3x10^{12}$
2	36.3	$5.1x10^{12}$

Thus, results show that the threshold voltage method can be used successfully in the electrolyte/sensor systems to determine the interface-state density in SOI-FET sensors.

4 Conclusion

In the study the Lim-Fossum model and the equivalent circuit for electrolyte/sensor system were used to derive the relationship between the threshold voltage of SOI- FET sensor and the voltage at the gate placed in electrolyte. This relationship and measured $V_{th1}(V_{tg})$ curve allow to estimate the state density D_{it2} at the sensor surface.

For calculating D_{it2} are required: 1) the device parameters, which can be determined with very good accuracy, and 2) the electrolyte parameters (associated with the charges in electrolyte and at the electrolyte/sensor surface), which are never precisely known for the real surface. It was shown that the errors associated with the uncertainty of parameters in electrolyte (with capacitances C_m and C_{ad}) are not critical in determination of D_{it2} for the commonly used parameters of the electrolyte/sensor system. The results are confirmed by measurements in solutions with the different concentration of ions.

The study was supported by Scientific Project of the Russian Academy of Science №0306-2018-0004.

References:

[1] F. Patolsky, G. Zheng, O. Hayden, M. Lakadamyali, X. Zhuang, C.M. Lieber, Electrical detection of single viruses,

Proceedings of the National Academy of Science of the United State of America, 2004, e3Vol.101, No.39, pp.14017-14022.

[2] F. Yang, G.J. Zhang, Silicon nanowire-transistor biosensor for study of molecule-molecule interactions, *Review Analytical Chemistry*, Vol.33, No.2, 2014, pp. 95–110.

[3] K-I. Chen, B-R. Li, Y-T. Chen, Silicon nanowire field-effect transistor-based biosensors for biomedical diagnosis and cellular recording investigation, *Nano Today*, Vol.6, No.2, 2011, pp.131-154.

[4] K. Zhu, Y. Zhang, Z. Li, Simultaneous detection of α-fetoprotein and carcinoembryonic antigen based on Si nanowire field-effect Transistors, *Sensors*, Vol.15, 2015, pp.19225-19236.

[5] Yu.D. Ivanov, T.O. Pleshakova, A.F. Kozlov, K.A Malsagova, N.V. Krohin, V.V. Shumyantseva, I.D. Shumov, V.P. Popov, O.V. Naumova, B.I. Fomin, D.A. Nasimov, A.L. Aseev, A.I. Archakov, SOI nanowire for the high-sensitive detection of HBsAg and α-fetoprotein, *Lab on a Chip*, Vol.12, No.23, 2012, pp.5104-5111.

[6] B. Veigas, E. Fortunato, P.V. Baptista, Field effect sensors for nucleic acid detection: recent advances and future perspectives, *Sensors*, Vol.15, 2015, pp.10380-10398.

[7] E. Dmitrienko , O. Naumova, B. Fomin, M. Kupryushkin, A. Volkova, N. Amirkhanov, D. Semenov, I. Pyshnaya, D. Pyshnyi, Surface modification of SOI-FET sensors for label-free and specific detection of short RNA analyte, *Nanomedicine*, Vol.11, No.16, 2016, pp. 2073-2082.

[8] O.V. Naumova, B.I. Fomin, D.A. Nasimov, N.V. Dudchenko, S.F. Devyatova, E.D. Zhanaev, V.P. Popov, A.V. Latyshev, A.L. Aseev, Yu.D. Ivanov, SOI nanowires as sensors for charge detection, *Semiconductor Science and Technology*, Vol.25, No.5, 2010, p.055004.

[9] O.V. Naumova, B.I. Fomin, Optimization of the Response of Nanowire Biosensors, *Optoelectronics, Instrumentation and Data Processing*, Vol.52, No.5, 2016, pp.1-5.

[10] H.-K. Lim, J. G. Fossum, Threshold Voltage ofThin-Film Silicon-on-Insularor (SOI) MOSFET's, *IEEE Transaction Electron Devices***,** Vol. ED-30, No.10, 1983, pp.1244-1251.

[11] D. E. Yates, S. Levine, T.W. Healy, Site-binding Model of the Electrolyte Double Layer at the Oxide/Wafer Interface, *Journal of the Chemical Society-Faraday Transactions*, Vol.70, 1974, pp.1807-1818.

[12] L. Bousse, N.F.de Rooij, P. Bergveld, Operation of chemically sensitive field-effect sensors as a function of the insulator-electrolyte interface, *IEEE Transactions on Electron Devices*, Vol. ED-30, No.10, 1983, pp. 1263-1270.

[13] A. Revil, P.W.J. Glower, Theory of ionic-surface electrical conduction in porous media, *Physical Review B*, Vol.55, No.3, 1997, pp.1757-1773.

[14] A.J. Bard, L.R. Faulkner, *Electrochemical methods: Fundamentals and Applications*, John Wiley & Sons, 2001.

[15] H. Wang, L. Pilon, Accurate Simulations of Electric Double Layer Capacitance of Ultramicroelectrodes, *The Journal of Physical Chemistry*,Vol.115, 2011, pp.16711-16719.

[16] D. Landheer, G. Aers, W.R. McKinnon, M.J. Deen, J.C. Ranuarez, Model for the field effect from layers of biological macromolecules on the gates of metal-oxide-semiconductor transistors, *Journal of Applied Physics*, Vol.98, 2005, p. 044701.

[17] A. Ortiz-Conde, F.J. Garcia Sanchez, J.J. Liou, A. Cerdeira, M. Estrada, Y. Yue, A review of recent MOSFET threshold voltage extraction methods, *Microelectronics Reliability*, Vol.42, No.4-5, 2002, pp.583-596.